



EXPERIMENTAL AND NUMERICAL APPROACHES: PERFORMANCE OPTIMIZATION OF A BAFFLED SOLAR CABINET DRYER FOR MANGO SLICES

Ermias A. Tesema^{1*}, Mulugeta A. Delele², Solomon W. Fanta³, Fentaw B. Masrie⁴, Melkamu
A. Workie⁵, Eneyw A. Tsegaye⁵

¹College of Engineering and Technology, Mattu University, Ethiopia

²Leibniz Institute for Agricultural Engineering and Bioeconomy, Potsdam, Germany

³Faculty of Chemical and Food Engineering, Bahir Dar University, Ethiopia

⁴Department of Food Science and Post-harvest, Oda Bultum University, Ethiopia

⁵College of Agriculture and Environmental Sciences, Bahir Dar University, Ethiopia

*Corresponding author email: ermiasa100@gmail.com

Abstract

During peak seasons, postharvest loss of mangoes remains a significant challenge for smallholder farmers in Ethiopia, driven by high production volumes, limited market access, and a lack of preservation methods. The objective of this research was to develop and enhance the performance of a solar cabinet dryer for mango slices through Computational Fluid Dynamics (CFD) simulations. A solar cabinet dryer incorporating a rectangular baffle solar collector was developed, built, and experimentally validated. The CFD simulation results showed a temperature difference of 4.35% and a relative humidity deviation of 7.8%, indicating good agreement with the experimental data. The model optimized the baffle design and inlet air velocity to maximize outlet temperature and minimize pressure drop. The optimal design was identified using Response Surface Methodology (RSM) in conjunction with ANSYS software. The best-performing configuration featured four baffles with 25% cut openings and an inlet air velocity of 1 m/s. The porous domain of mango slices was incorporated into the model to predict moisture transport with experimental effective diffusivity of $(5.224 \times 10^{-7} \text{ m}^2/\text{s})$. Results showed that the designed dryer achieved uniform temperature and moisture distribution, with higher drying rates observed near the lower trays. The moisture content in mango slices was reduced from 45942.17 mol/m³ to 2,677 mol/m³ within two hours of drying. The CFD model showed strong predictive accuracy with only

Received May 28, 2025; **Revised**: June 11, 2025; **Accepted**: July 25, 2025; **Published**: August, 2025.

Corresponding author- Ermias A. Tesema



minor discrepancies observed in the simulation of temperature, relative humidity, and moisture movement. The developed dryer offers a sustainable and cost-effective solution to mitigate postharvest mango losses, featuring an efficient design that enhances food security and improves farmer livelihoods.

Keywords: CFD modeling, heat and mass transfer, mango slices, postharvest loss, solar dryer

I. INTRODUCTION

Postharvest losses of fruits, particularly mangoes, continue to pose a serious challenge for smallholder farmers in Ethiopia. Although mangoes are highly valued for their nutritional benefits and economic importance, they often experience significant post-harvest losses due to insufficient preservation and processing techniques, particularly during peak production seasons. The Food and Agriculture Organization (FAO) estimates that in developing nations, up to 40% of perishable goods may be lost, undermining food security and reducing the earnings of agricultural producers [1].

Solar drying offers a sustainable and cost-efficient alternative to conventional drying approaches, enhancing energy efficiency and minimizing dependence on fossil fuels. Nevertheless, its performance is sometimes hindered by challenges such as uneven temperature distribution, low efficiency, considerable energy losses, and inadequate airflow—factors that adversely affect drying time and product quality[2].

Computational Fluid Dynamics (CFD) has emerged as a powerful analytical tool in both academic research and industrial applications for studying fluid flow behavior and thermal processes in drying systems. Recent progress in CFD techniques has empowered researchers to more effectively design and optimize solar dryers. This, in turn, has led to enhanced thermal performance, energy efficiency, and drying uniformity. CFD provides a detailed understanding of heat and mass transfer phenomena, enabling the prediction and enhancement of drying conditions within solar dryers. Studies have demonstrated the potential of baffled solar collectors to enhance airflow and temperature distribution, thereby improving drying efficiency [3].



This study focuses on designing and optimizing a solar cabinet dryer equipped with baffles for mango slices through CFD modeling, targeting issues of uneven drying and energy loss. The results are intended to advance solar drying technology, improve mango preservation methods, and contribute to strengthening food security in Ethiopia.

II. MATERIALS AND METHODS

A. Development, Fabrication, and Field Evaluation of the Dryer

The study was conducted at the Bahir Dar Institute of Technology, Bahir Dar University, located in northwestern Ethiopia. The solar dryer was constructed from materials such as MDF wood, glass, sheet metal, black paint, and mesh trays. Equipment used included a digital balance, Lux meter, anemometer, data loggers, photovoltaic (PV) system, colorimeter, refractometer, and caliper. Computational Fluid Dynamics (CFD) simulations were performed using ANSYS Workbench version 18.0.

B. CFD Simulation of the Solar Cabinet Dryer

Accurate experimental setup, validation, and optimization are essential for effective CFD modeling aimed at enhancing design and performance [4]. The study involved the design, modeling, simulation, and optimization of solar cabinet dryers by varying the number of baffles, baffle cut dimensions, and air velocity, as outlined in Table I.

TABLE I: Collector configurations

Flat plate collector	Flat plate collectors with	
without baffle	Baffle cut	Number of baffles
	25%	2,4,6
	37.5%	2,4,6
	50%	2,4,6

ANSYS CFX 18.1 was used to model fluid transport in the dryer, testing solar collectors with and without baffles. Mango slices were modeled as a 3 mm porous medium (Fig. 1).

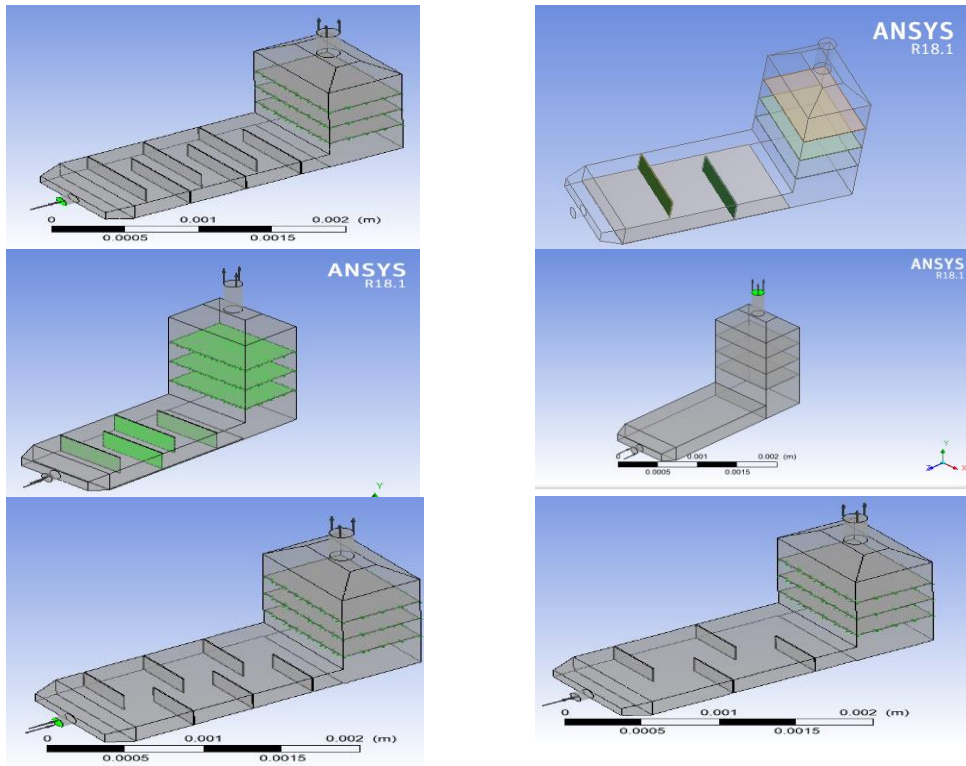


Fig. 1: Solar cabinet dryers with 0, 2, 4, and 6 baffles with baffle cut of (25%-50%)

The turbulent airflow in the drying system was modeled by the standard Reynolds-averaged Navier-Stokes equations, complete with energy transport equations using equations 1-3.

$$\frac{\partial \rho}{\partial t} + \nabla \cdot (\rho \vec{v}) = 0 \quad \text{Equation 1}$$

$$\frac{\partial}{\partial t} (\rho \vec{v}) + \nabla \cdot (\rho \vec{v} \vec{v}) = -\nabla p + \nabla \cdot (\bar{\tau}) + \rho \vec{g} + \vec{F} \quad \text{Equation 2}$$

$$\frac{\partial}{\partial t} (\rho E) + \nabla \cdot (\vec{v} (\rho E + p)) = \nabla \cdot [-\vec{q} + \sum_j h_j \vec{f}_j + (\bar{\tau} \cdot \vec{v})] \quad \text{Equation 3}$$

Where

\vec{v} = is the fluid velocity vector and

ρ = is the density of air

\vec{F} = is the source term for momentum

E = is the total energy, $\bar{\tau}$ = stress tensor

1) *Geometry and Meshing Setup*: The three-dimensional model shown in Fig. 2 was discretized using the finite volume approach and meshed with tetrahedral elements in ANSYS-CFX, applying mesh refinement in key regions.

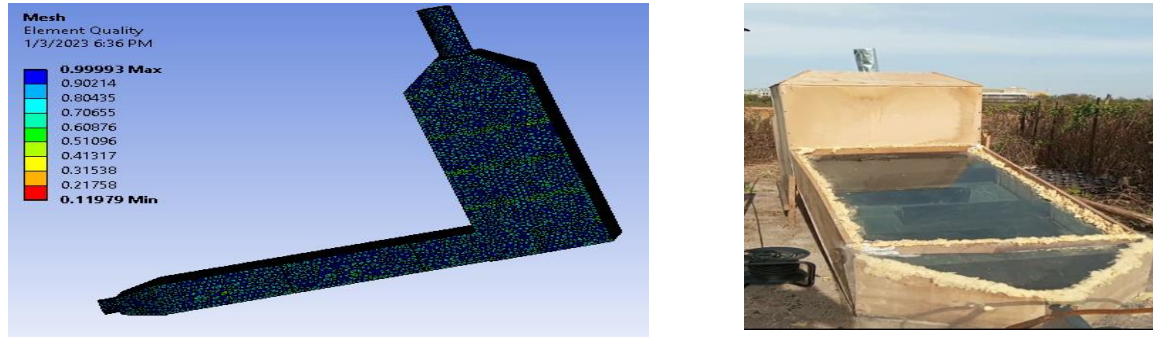


Fig. 2: Computational mesh of the solar dryer alongside the fabricated prototype.

2) *Model setup and boundary conditions*: In this study, the boundary conditions were defined as a function of the meteorological conditions of Bahir Dar and informed by prior experimental results, as summarized in Table II.

TABLE II: Model setup and boundary conditions

Parameter	Type	Value and unit
Solar radiation	Daily ambient	$-26.924t^2 + 279.54t + 259.33, R^2 = 0.9827$
Inlet temperature (for transit simulation)	Ambient	$4e-8t^2 + 0.0012t + 19.57$
Inlet air velocity	normal	2m/s for experiment and 1-4(m/s)
Wall	wood (MDF)	0.018m
Collector	sheet metal	0.008m
Glass	window glass	4mm, transparent
Baffle	sheet metal	0.008m
Porous(product)	Mango	3.88kj/(kg k)



3) *Turbulence model*: Among various turbulence models, the standard SST (Shear Stress Transport) model was selected due to its suitability for capturing swirling flow characteristics [5].

4) *Sensitivity Analysis*: Given that the outlet temperature was a critical outcome of interest in the simulation, the mesh independence study was carried out by analyzing variations in this parameter across different mesh densities.

5) *Model Validation*: To validate the simulation results, the outlet temperature predicted by the CFD model was compared with the experimentally measured outlet temperature. The accuracy of the model was assessed using the Percent Bias (PBIAS) statistical metric, which quantifies the average tendency of the simulated values to deviate from the observed data. A lower PBIAS value indicates a better agreement between the model and experimental results. The PBIAS was calculated using the following equation (Parajuli et al., 2009) as shown in equation 4.

$$\text{PBIAS} = \frac{\sum_{i=1}^N (T_{\text{expi}} - T_{\text{prei}}) * 100}{\sum_{i=1}^N T_{\text{expi}}} \quad \text{Equation 4}$$

Where:

T_{expi} is the experimental outlet temperature at time step i ,

T_{prei} is the predicted outlet temperature from the model at time step i , and

N is the total number of data points.

6) *Drying Temperature, Velocity, and Relative Humidity Distribution*: A CFD model was developed to simulate temperature, pressure, velocity, and relative humidity by solving the RANS equations alongside turbulence models, incorporating supplementary expressions for saturation pressure (p^{sat}) and relative humidity as given in Equations 5 and 6 [6].

$$\ln(p_{\text{sat}}) = A - \left(\frac{B}{T + C} \right) \quad \text{Equation 5}$$

Where A , B , and C are constants specific to water 16.3872, 3885.70, and 230.170, respectively.

$$\text{RH} = \left(\frac{P}{P_{\text{sat}}} \right) * 100 \quad \text{Equation 6}$$

7) *Optimization of the Developed Model*: Following the parameter studies, an optimized design, considering air velocity, baffle cut dimensions, and the number of baffles, was developed to maximize the outlet temperature while minimizing pressure drop. This tailored design was



further refined using the Response Surface Methodology (RSM) optimization tool available within the ANSYS software.

TABLE III: Optimization parameters and their levels

Parameter	Units	Levels	L1	L2	L3	L4
Velocity of air	m/s	4	1	2	3	4
Baffle cut	%	3	25	37.5	50	55
No. of baffles	N	3	2	4	6	

8) *Simulation of Moisture Movement*: In solar dryers, water vapor is treated as a scalar property, independently solving its mass transport with a general conservation equation without affecting mass, momentum, and energy solutions for dry air.

$$\frac{\partial(\rho w)}{\partial t} = \nabla \cdot (\rho \vec{u} w) = \nabla \cdot (\rho D) + S_w \quad \text{Equation 7}$$

Where w is the humidity ratio (kg water vapor/kg dry air) and D is the water vapor diffusion coefficient, which depends on temperature, the moisture transfer between mango slices and air during drying is represented by S_w determined by equation 8

$$S_w = M_w = A_{sv} h_m (C_e - C_a) \quad \text{Equation 8}$$

The source term S_w is added corresponding to the moisture transfer between the mango slices and air during drying. The equivalent water vapor concentration of the mango slices and the water vapor concentration of the air are given by the following equations 9 (a and b).

$$C_e = \frac{M_w P_{sat} a_w}{RT} \quad (a) \quad C_a = \frac{M_w P_{sat} RH}{RT} \quad (b) \quad \text{Equation 9}$$

$$\rho_s = \frac{D_{eff}}{L_s}, \quad RH = \frac{P_a}{P_{sat}} \quad \text{Equation 10}$$



The overall mass transfer coefficient $\frac{1}{h_m} = \frac{1}{h_s}$ Where h_m = surface mass transfer coefficient(m/s) As_v is the ratio of the mango slice's surface area to volume $D_{eff} = 5.224 \times 10^{-7} \text{ m}^2/\text{s}$ calculated from the previous experimental study [7].

The moisture source term was determined based on the rate of change of moisture content during the drying process. This rate depends on the mass transfer coefficient (km) and the difference between concentrations of water vapor at the outer surface of mango slices, C_e , and in the surrounding air, C_a . p_a is the vapor pressure and p_{sat} is the saturation vapor pressure of free water. Antoine's equation was used to calculate the saturation vapor pressure as a function of temperature.

$$p_{sat} = \exp \left(A - \frac{B}{T + C - 273} \right) \quad \text{Equation 11}$$

Determination of mass transfer coefficient

The heat transfer coefficient was calculated using the Chilton–Colburn analogy for thermal and concentration boundary layers, as described in [8].

$\frac{D_{eff}}{k}$ K is the mango thermal conductivity = 0.925 W/m·°C. Initial Moisture content (82.75%) in (mol/m³) = $MC = \frac{MW}{M_{mango}}$ the initial moisture content of the product was calculated as 45942.17 (mol/m³) with a total of 6kg of mango slices.

9) *Thin-Layer Drying Model*: In the simulation of the mango slice drying process, the Page model was adopted to describe the thin-layer drying kinetics due to its proven accuracy in modeling the drying behavior of fruits and vegetables [9]. The model is expressed as:

$$MR = \exp(-kt^n)$$

where:

MR is the moisture ratio (dimensionless),

k is the drying rate constant (1/min),

t is the drying time (min), and

n is a dimensionless empirical constant.



The parameters k and n were obtained from previous experimental studies on mango drying under similar conditions. This model was integrated into the simulation to predict the moisture removal rate from mango slices during drying, providing a more realistic representation of the drying curve. The use of the Page model enhances the accuracy of simulation outputs by aligning them closely with observed drying behavior.

III. MODEL SIMULATION RESULTS

A. Mesh Independent Study Result

Meshing is crucial for accurate modeling, as results must remain consistent regardless of mesh size. To ensure precision, the optimal number of nodes and elements should be identified, where further refinement does not significantly impact the results.

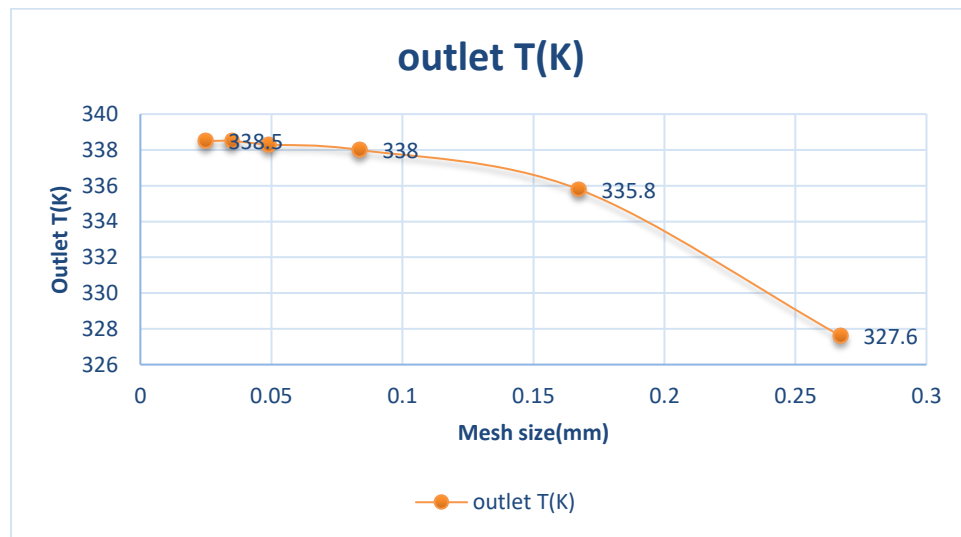


Fig. 3. Mesh independent based on mesh size on the outlet temperature

From the mesh independent study (Fig. 3), the mesh size with 0.048992mm and 82,793, 18,963 numbers of elements and nodes, respectively, was selected for further study.



B. Model Validation

The CFD model overestimated the tray temperature by 2.176°C (4.35%) compared to the experimental part of this research [7] due to unaccounted heat losses. The moisture distribution also underestimated the experimental value by 7.8%, as shown in Fig. 4.

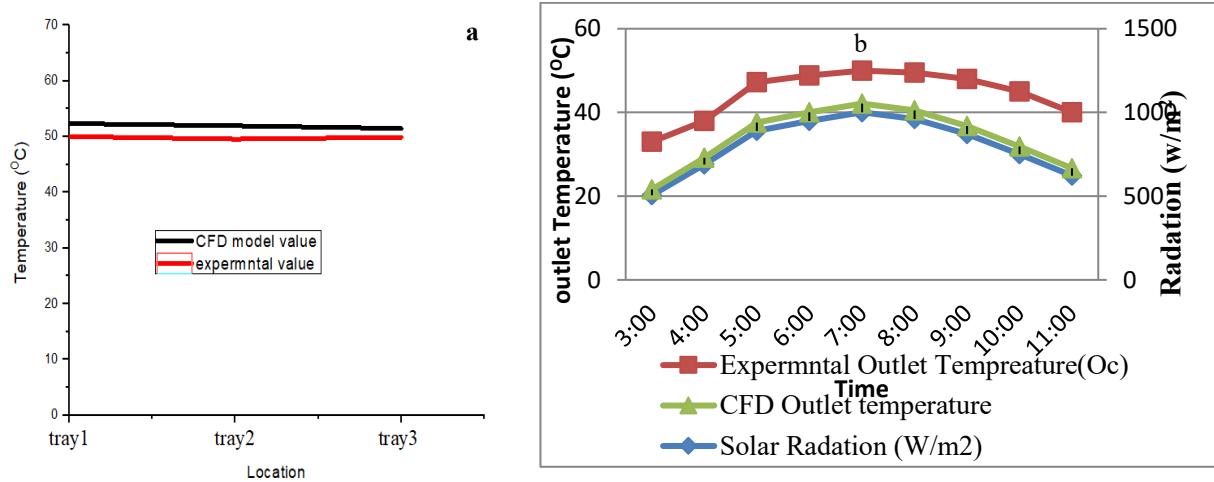


Fig. 4. Validation graph based on the location of outlet T (°C) (a) and daily temperature variation (transit simulation) (b)

C. Pressure, Temperature, and Velocity Distribution

Efficient solar dryer operation depends on short drying time and uniform air velocity, temperature, and moisture distribution [2]. Figures 6-7 show velocity streamlines and temperature distribution. A maximum velocity of 4 m/s and pressure of 22 Pa ensured uniform airflow in the drying chamber. High velocity and pressure at the inlet and outlet were attributed to the narrow cross-section. The absorber temperature peaked at 338.2 K, while tray 1 reached 365.2 K, indicating improved thermal performance due to the rectangular baffled solar collector, Fig. 5 (a and b).

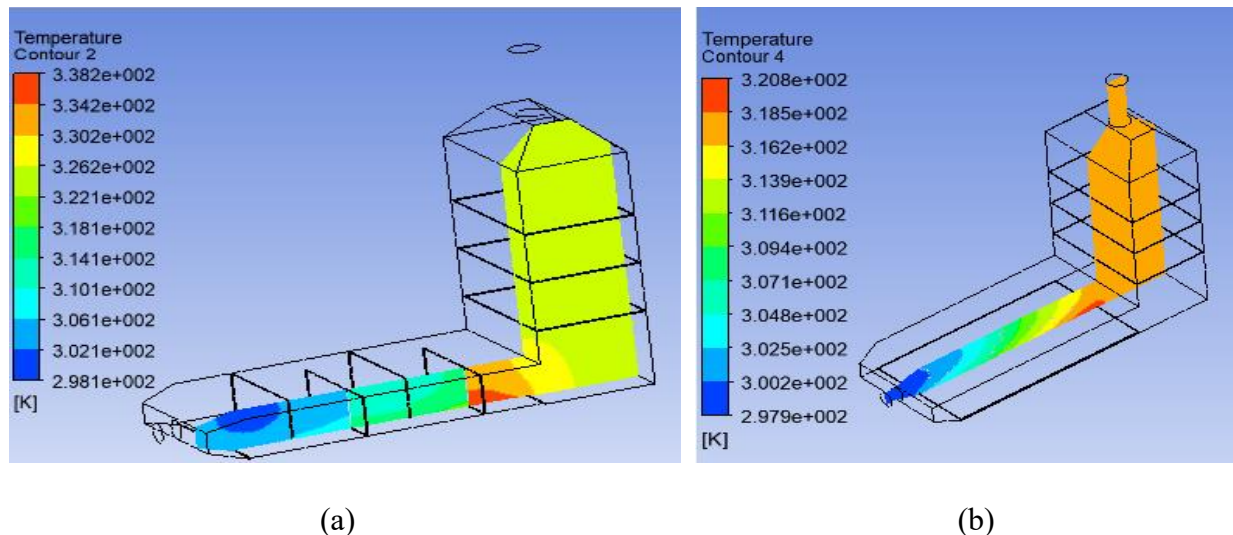


Fig. 5.: Temperature distribution inside the baffled collector and collector without baffle: a- collector with baffle, b-collector without baffle

As shown in the Fig. 5 simulation results, the solar cabinet dryer integrated with a rectangular baffle showed that the overall drying output temperature in the location of tray 1 was increased by 7.403°C(14%) than the non-baffled one. Solar collector with rectangular baffles improves the circulation of air within the collector, resulting in a more efficient transfer of energy from the heated metal sheet to the humid air. Based on this validation, the optimization of solar dryers was done with solar cabinet dryers integrated with rectangular baffles.

D. Velocity and Temperature Distribution

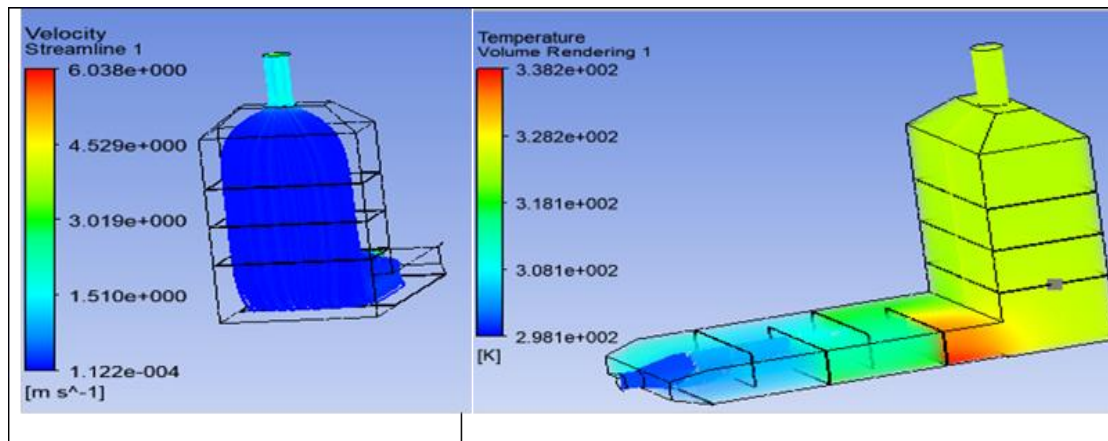


Fig 6. Velocity and temperature distribution on the designed solar dryer

Fig. 6 shows higher temperatures at the bottom of the collector compared to near the cover, with slight temperature variation in the chamber. The CFD model indicated an even distribution of heated air (50-54°C), contributing to faster, well-dried mango slices, as noted by [2].

E. Relative Humidity Distribution

Relative humidity (RH) measures the moisture in the air relative to its maximum capacity at a given temperature. In the dryer, heated air reduces RH. The CFD model showed RH in the chamber at 17.5%, close to the experimental value of 19%, with a 7.8% error, indicating acceptable accuracy for parametric surveys.

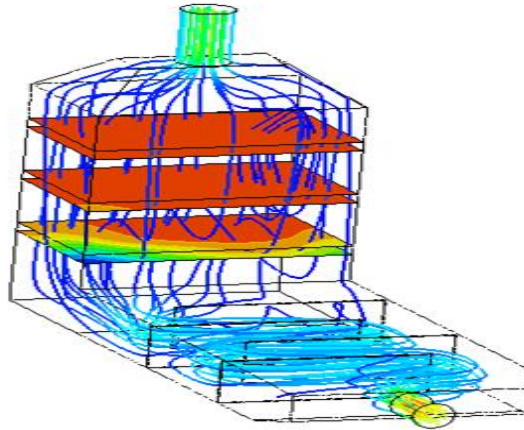


Fig. 7: Relative humidity distribution inside the dryer (counterplot with mango slices loading)

F. Improving Dryer Efficiency Using CFD Simulations

The outlet temperature of the solar collector is key to improving product quality and reducing drying time. Maintaining an optimal pressure drop is essential for minimizing energy consumption and ensuring cost-effective operation.

1) Development of Regression Model Equation: The model equations correlating pressure drop (2FI model) and outlet temperature (quadratic model) to process variables are provided in equations 12 and 13.

$$\text{Temperature(K)} = 315.41 - 15.35 * A - 5.69 * B + 3.27 * C[1] - 1.64 * C[2] + 5.28 * AC[1] - 2.83 * AC[2] - 3.76 * BC + 18.7 * A^2 - 6.16 * B^2 \quad \text{Equation 12}$$

Pressure drop (pa)

$$= 29.45 + 17.26 * A - 5.32 * B - 13.01C1 - 3.97 * C2 - 12.5 * AC1 - 4.88 * AC2 + 2.09 * BC \quad \text{Equation 13}$$

The regression model estimates temperature and pressure drop based on air velocity (A), baffle cut (B), and number of baffles (C). Temperature decreases with higher air velocity and baffle cut, while it increases with more baffles and the interaction of A and C. Pressure drop increases with air velocity but decreases with higher baffle cut and fewer baffles. Coefficients indicate the



strength and direction of these effects, with C1 and C2 representing binary interactions using 6 baffles as a reference.

G. Study of Desirability

The objective of this study is to find the best configuration of the baffle (baffle cut and baffle number) and velocity of air to maximize the outlet temperature while minimizing the pressure drop.

TABLE IV: Constraints for optimization of the collector

Name	Goal	Lower Limit	Upper Limit	Lower Weight	Upper Weight	Importance
A: velocity of air	is in range	1	4	1	1	3
B: Baffle cut	is in range	25	50	1	1	3
C: Number of baffles	is in range	2	6	1	1	3
Temperature	maximize	306	350.6	1	1	3
pressure drop	minimize	2.1	88.52	1	1	3

TABLE V: Optimized solutions for combinations of numerical and categorical factor levels

Number	velocity of air	number of baffles	baffle cut	Temperature	pressure drop	Desirability
1	1.000	4	25	350.929	3.0896	0.994 Selected

Based on the optimization, it can be concluded that the best response for attaining maximum outlet temperature and minimum pressure drop was obtained by setting the velocity of air at 1m/s, the number of baffles at 4, and the baffle cut at 25%. These parameters were found to be the optimal

values for achieving the desired outcome of the experiment with maximum outlet temperature (77°C) at the outlet of the collector and 58°C on tray 1.

H. Moisture Distribution within Trays

Using a detailed geometry and mesh, simulations of airflow, heat transfer, and moisture transport were conducted for the tray dryer. As shown in Fig. 8, the simulated moisture distribution within the porous mango slices after 2 hours of drying revealed a significant reduction in moisture content—from $45,942.17\text{ mol/m}^3$ to $2,677\text{ mol/m}^3$, for slices with a thickness of 3 mm.

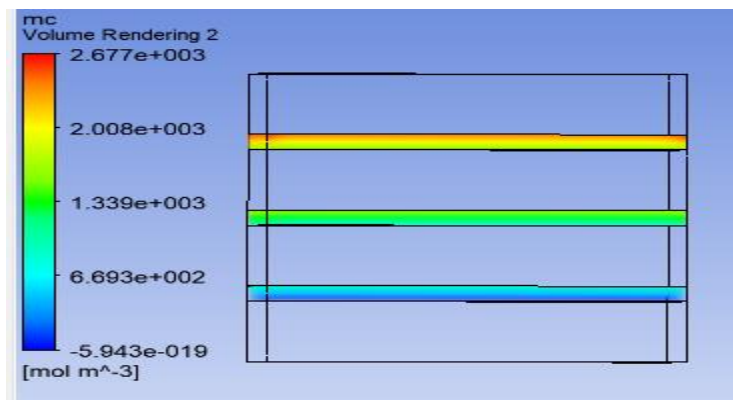


Fig.8. Moisture content in 3 mm thick mango slices significantly decreased after 2 hours of simulation.

IV. CONCLUSION AND RECOMMENDATION

A. Conclusion

This study successfully developed and optimized a baffled solar cabinet dryer for mango slices using Computational Fluid Dynamics (CFD) modeling. The integration of rectangular baffles significantly enhanced airflow distribution, temperature uniformity, and drying efficiency. The CFD simulations, validated against experimental data, demonstrated high predictive accuracy with minimal deviations, 4.35% in temperature and 7.8% in relative humidity. Optimal drying conditions were achieved with an air velocity of 1 m/s, four baffles, and a 25% baffle cut, resulting in enhanced thermal performance and minimized pressure drop. The drying system effectively



reduced mango moisture content from 45,942.17 mol/m³ to 2,677 mol/m³ within two hours, confirming its potential as a sustainable and cost-effective solution to reduce postharvest losses and enhance food security. The model also established a strong foundation for further scaling and adaptation to other perishable crops. This finding is particularly significant for our community, especially in mango-producing regions like Arba Minch, as it offers a practical, low-cost solution to reduce postharvest losses, improve food preservation, and support smallholder farmers through enhanced drying technology.

B. Recommendations

Future studies should aim to boost the dryer's thermal efficiency by reducing heat losses and assessing its scalability for larger capacities. Incorporating full moisture transport modeling with high-performance computing (HPC) is also recommended to capture transient heat and mass transfer within mango slices. This approach would enhance the prediction of drying behavior and support the design of more efficient dryers for a range of perishable crops and climates.

REFERENCES

- [1]. J. Gustavsson, C. Cederberg, U. Sonesson, R. van Otterdijk, and A. Meybeck, "*Global Food Losses and Food Waste: Extent, Causes and Prevention*," Food and Agriculture Organization of the United Nations, Rome, Italy, 2011.
- [2]. E. Getahun, M. A. Delele, N. Gabbiye, S. W. Fanta, P. Demissie, and M. Vanierschot, "Importance of integrated CFD and product quality modeling of solar dryers for fruits and vegetables: A review," *Solar Energy*, vol. 220, pp. 88–110, May 2021.
- [3]. A. Khanlari, H. Ö. Güler, A. D. Tuncer, C. Şirin, Y. C. Bilge, Y. Yılmaz, and A. Güngör, "Experimental and numerical study of the effect of integrating plus-shaped perforated baffles to solar air collector in drying application," *Renewable Energy*, vol. 145, pp. 1677–1692, Jan 2020.
- [4]. W. L. Oberkampf and T. G. Trucano, "Verification and validation in computational fluid dynamics," *Progress in Aerospace Sciences*, vol. 38, no. 3, pp. 209–272, April 2002.

Received May 28, 2025; **Revised**: June 11, 2025; **Accepted**: July 25, 2025; **Published**: August, 2025.

Corresponding author- Ermias A. Tesema



- [5]. J. M. Gorman, E. M. Sparrow, J. P. Abraham, and W. J. Minkowycz, "Evaluation of the efficacy of turbulence models for swirling flows and the effect of turbulence intensity on heat transfer," *Numerical Heat Transfer, Part B: Fundamentals*, vol. 70, no. 6, pp. 485–502, Nov 2016.
- [6]. K. Song, C. Jeong, J. Nam, and C. Han, "Hybrid compressor model for optimal operation of compressed dry air system in LCD production industry," *Industrial & Engineering Chemistry Research*, vol. 51, no. 13, pp. 4998–5002, March 2012.
- [7]. E. A. Tesema, "Design, Development, and Performance Evaluation of Baffled Solar Mango Slice Dryer," Ph.D. dissertation, Department of Agricultural Engineering, Jimma University, Jimma, Ethiopia, 2024.
- [8]. A. Pasban, H. Sadrnia, M. Mohebbi, and S. A. Shahidi, "Spectral method for simulating 3D heat and mass transfer during drying of apple slices," *Journal of Food Engineering*, vol. 212, pp. 201–212, Nov 2017.
- [9]. I. T. Togrul and D. Pehlivan, "Modeling of thin layer drying kinetics of some fruits under open-air sun drying process," *Journal of Food Engineering*, vol. 65, no. 3, pp. 413–425, Dec 2004.